

Distinct fibroblast lineages determine dermal architecture in skin development and repair.

Driskell, RR; Lichtenberger, BM; Hoste, E; Kretzschmar, K; Simons, BD; Charalambous, M; Ferron, SR; Herault, Y; Pavlovic, G; Ferguson-Smith, AC; Watt, FM

2013 Macmillan Publishers Limited. All rights reserved

For additional information about this publication click this link.

<http://qmro.qmul.ac.uk/xmlui/handle/123456789/12514>

Information about this research object was correct at the time of download; we occasionally make corrections to records, please therefore check the published record when citing. For more information contact scholarlycommunications@qmul.ac.uk

Published in final edited form as:

Nature. 2013 December 12; 504(7479): 277–281. doi:10.1038/nature12783.

Distinct fibroblast lineages determine dermal architecture in skin development and repair

Ryan R. Driskell^{1,5}, Beate M. Lichtenberger^{#1,5}, Esther Hoste^{#3,5}, Kai Kretzschmar^{#1,5}, Ben D. Simons⁶, Marika Charalambous², Sacri R. Ferron², Yann Herault⁴, Guillaume Pavlovic⁴, Anne C. Ferguson-Smith², and Fiona M. Watt^{1,3,5,*}

¹Wellcome Trust Centre for Stem Cell Research, University of Cambridge, Cambridge CB2 1QR, UK.

²Department of Physiology, Development & Neuroscience, University of Cambridge, Cambridge CB2 3EG, UK.

³Cancer Research UK Cambridge Research Institute, Li Ka Shing Centre, Robinson Way, Cambridge CB2 0RE, UK.

⁴Institut Clinique de la Souris, Parc d'Innovation, 67404 Illkirch-Grattenstaden, Cedex, France

⁵Centre for Stem Cells and Regenerative Medicine, King's College London, 28th floor, Tower Wing, Guy's Hospital, London SE1 9RT, UK

⁶Department of Physics, Cavendish Laboratory, University of Cambridge, CB3 0HE

These authors contributed equally to this work.

Abstract

Fibroblasts are the major mesenchymal cell type in connective tissue and deposit the collagen and elastic fibers of the extracellular matrix (ECM)¹. Even within a single tissue fibroblasts exhibit remarkable functional diversity, but it is not known whether this reflects the existence of a differentiation hierarchy or is a response to different environmental factors. Here we show, using transplantation assays and lineage tracing, that the fibroblasts of skin connective tissue arise from two distinct lineages. One forms the upper dermis, including the dermal papilla that regulates hair growth and the arrector pili muscle (APM), which controls piloerection. The other forms the lower dermis, including the reticular fibroblasts that synthesise the bulk of the fibrillar ECM, and the pre-adipocytes and adipocytes of the hypodermis. The upper lineage is required for hair follicle formation. In wounded adult skin, the initial wave of dermal repair is mediated by the lower lineage and upper dermal fibroblasts are recruited only during re-epithelialisation. Epidermal beta-catenin activation stimulates expansion of the upper dermal lineage, rendering wounds permissive for hair follicle formation. Our findings explain why wounding is linked to formation of ECM-rich scar tissue that lacks hair follicles²⁻⁴. They also form a platform for discovering fibroblast lineages in other tissues and for examining fibroblast changes in ageing and disease.

Users may view, print, copy, download and text and data- mine the content in such documents, for the purposes of academic research, subject always to the full Conditions of use: http://www.nature.com/authors/editorial_policies/license.html#terms

*Correspondence and requests for materials should be addressed to (fiona.watt@kcl.ac.uk; +44 20 7188 5608).

Author Contributions RRD and FMW designed the experiments, performed data analysis, interpreted the results, and wrote the manuscript. BML, EH, KK, ACF, SRF, BDS and MC assisted in performing and designing experiments, analyzing data, and interpreting results. YH and GP generated the Dlk1CreERT transgenic mouse.

Supplementary information line Supplementary information can be found in the accompanying PDF file.

Author Information Reprints and permissions information is available at www.nature.com/reprints.

The authors have no competing financial interests.

At E12.5 mouse epidermis comprises one or two cell layers and the dermis appears homogeneous in composition (Fig. 1a)⁵. By E18.5 the epidermis is fully stratified, hair follicles, with associated DP, are forming and the upper (papillary) dermis is distinguishable from the lower (reticular) dermis because of its higher cellular density (Fig. 1a). By P2 the hypodermis has formed, comprising differentiated adipocytes and pre-adipocytes (Fig. 1a). We identified markers of different fibroblast subpopulations at each developmental stage, based on prior studies^{6,7} and the availability of antibodies for live cell sorting.

The pan-fibroblast marker platelet derived growth factor receptor alpha (PDGFRa) is expressed in upper and lower dermis at all stages of development (Fig. 1b)⁸. In contrast there were temporal and spatial changes in expression of 18 other fibroblast markers (Fig. 1b-c; Fig. E1-3). From E16.5 CD26 and B lymphocyte induced maturation protein (Blimp1/Prdm1) were selectively expressed in the upper dermis, while Sca1 was selectively expressed in the lower dermis. Delta-like homologue 1 (Dlk1) and Lrig1 were expressed throughout the dermis at E12.5, with Dlk1 expression persisting in the lower dermis from E18.5 and Lrig1 expression persisting in the upper dermis. The changes in abundance of CD26+, Sca1+ and Dlk1+ cells were confirmed by flow cytometry of GFP+ dermal cells from PDGFRaH2BeGFP mice⁸ (Fig. E3). Several of the markers were also differentially expressed in neonatal human skin (Fig. E4).

To evaluate the differentiation potential of different dermal fibroblasts (Fig. 2a), cells were flow sorted from P2 PDGFRaH2BeGFP dermis⁸ (Fig. E5c-e), combined with unlabelled epidermal and dermal cells and injected into chambers implanted into nude/BalbC mice⁹. Papillary dermal cells (CD26+Sca1-) contributed exclusively to the upper dermis (Fig. 2b-d; Fig. E6a), including the dermal papilla and APM (Fig. 2, e, f). Hypodermal fibroblasts (Dlk1+Sca1+ and Dlk1-Sca1+) differentiated into adipocytes but not into APM or dermal papilla (Fig. 2b-d, Fig. E6c, d). Dlk1+Sca1- cells, located primarily at the boundary between reticular dermis and hypodermis (Fig. E5a, b), contributed to all dermal mesenchymal compartments (Fig. 2b-d, Fig. E6b). However, while we cannot rule out the existence of multipotent fibroblasts in adult skin, Dlk1+Sca1- cells did not persist after P10, when Dlk1 was no longer expressed in the dermis (Fig. E4d and data not shown).

The number of hair follicles was higher in grafts containing upper dermal (CD26+Sca1-) cells than Dlk1-Sca1+ hypodermal cells (Fig. E6e-i). Dlk1-Sca1+ cells are a subpopulation of Lin-CD34+CD29+Sca1+ adipocyte precursors, which also express Pdgfra (Fig. E5f-i)¹⁰. To establish whether hypodermal cells were less effective at supporting hair follicle formation we compared control grafts containing unfractionated P2 PDGFRaH2BeGFP+ cells with grafts in which we excluded papillary/reticular cells (CD26+/Dlk1+/Sca1- cells depleted) or reticular/hypodermal cells (Dlk1+/-Sca1+ cells depleted) (Fig. 2g-k; Fig. E6j-l). Since CD26, Dlk1 and Sca1 are not expressed in the DP (data not shown) all grafts contained DP cells. The contribution of GFP+ cells to the grafts was extensive in all cases (Fig. 2i). Hair follicle formation was similar in the grafts of unfractionated dermal cells and those depleted of reticular and hypodermal cells. In contrast, when the papillary and reticular dermal cells were excluded very few hair follicles formed (Fig. 2h-k). Thus P2 skin contains cells that are restricted to forming either the upper or lower dermal lineages on skin reconstitution, the upper dermal cells being required for hair follicle formation.

We next performed lineage tracing with specific promoters. We crossed Dlk1CreER mice with Rosa-CAG fl/stop/fl tdTomato mice, then labelled with Tamoxifen at E12.5 (when all fibroblasts are Dlk1+; Fig. 1c) or E16.5 (when only reticular fibroblasts express Dlk1; Fig. 1c) and harvested at P2 or P21 (Fig. 3a-k). Flow cytometry established that the labelling efficiency was over 95% (Fig. E7a-c). When Dlk1 expressing cells were labelled at E12.5 all of the dermal mesenchymal compartments (Pdgfra+) were labelled (Fig. 3a-d). In contrast,

when cells were labelled at E16.5 the only labelled fibroblasts were reticular and hypodermal cells, including mature adipocytes (Fig. 3e-k). Therefore after E16.5 dermal fate restriction occurs, such that cells expressing *Dlk1* only give rise to the lower dermal lineages. We confirmed this by examining adipogenesis of dermal cells in culture (Fig. E3d-g; see Supplementary Information)^{6,11}.

We next performed lineage tracing with *Blimp1Cre*. Between E16.5 and E18.5 *Blimp1* was expressed in the DP, dermal sheath and papillary dermis (Fig. 1c; Fig. E7d-e)^{12,13}, but from P2 through adulthood dermal *Blimp1* expression was confined to the DP and dermal sheath (Fig. E7f-g). *Blimp1* expressing epidermal and endothelial cells (Fig. E7h-i)¹³⁻¹⁵ were excluded from analysis based on co-expression of relevant markers. The fidelity of the *Blimp1* promoter was established by flow sorting (Fig. E7j-k).

At all time points DP and dermal sheath cells were labelled in *Blimp1Cre* x *CAGCATeGFP* mice (Fig. 3l-o). At E16.5 the papillary dermis was unlabeled (Fig. 3l), but at E18.5 the papillary dermis contained GFP positive cells, consistent with the pattern of endogenous *Blimp1* expression (Fig. E7e, h). From P14 onwards all APM were GFP positive and only a few GFP+ cells remained in the papillary dermis (Fig. 3n, o). Thus P2 papillary dermal fibroblasts are the progenitors of the APM. Labeled papillary fibroblasts never contributed to the reticular dermis or hypodermis.

We used *Lrig1* as an additional marker for lineage tracing¹⁶ (Fig. 1c; Fig. 3r-u; Fig. E7l-q). The specificity of the *Lrig1-GFP-IRES-CreER* reporter line¹⁷ was confirmed by flow cytometry (Fig. E7n). P2 dermal cells from *Lrig1-GFP-IRES-CreER* x *Rosa-CAG fl/stop/fl* *tdTomato* crosses treated with Tamoxifen at E16.5 expressed PDGFRa and CD26 but not *Sca1* (Fig. E7n-q). At P2 labelling was restricted to the papillary dermis (Fig. 3r, Fig. E7m). At P21 the APM and papillary dermis were labelled, while the reticular dermis and fat were unlabelled (Fig. 3s-u). Our data suggest that loss of papillary dermis after the first hair follicle cycle^{8,18} is due to differentiation of papillary fibroblasts into the APM, which was further confirmed by clonal analysis in *PDGFRaCreER* x *CAGCATeGFP* mice (Fig. E8). It is interesting that the papillary dermis is more pronounced in human skin, which has fewer hair follicles and therefore fewer APM, than mouse skin⁵. We conclude that from E16.5 the developing dermis undergoes fate restriction such that cells in the upper dermis that express *Lrig1* or *Blimp1* give rise to the DP, APM and papillary fibroblasts, while *Dlk1*-positive cells in the lower dermis give rise to the reticular dermis, hypodermis and adipocyte layer (Fig. 3v, w).

To investigate how fibroblasts of different lineages contribute to skin repair, we created full thickness wounds in adult back skin. We ruled out any contribution of bone marrow derived cells to the *Pdgfra*+ dermal compartment (Figure E9a-k; Supplementary Information). When *PDGFRaCreER* x *lox/stop/lox* *tdTomato* mice that had been injected with Tamoxifen at E17.5 were wounded in adulthood, we found *tdTomato*+ cells throughout the repairing dermis (Fig. E9l-n). When we examined wound healing in *Dlk1CreER* x *lox/stop/lox* *tdTomato* mice that had been injected with Tamoxifen at E16.5 to selectively label the lower dermis (Fig. 4a-c; Fig. E10a, b), a large proportion of wound fibroblasts, including cells that expressed the myofibroblast marker alpha-smooth muscle actin¹⁹ (Fig. E10b), were *tdTomato*-positive (Fig. 4b-c). In adult skin of *Blimp1Cre* x *lox/stop/loxGFP* mice only upper dermal fibroblasts and CD31-positive endothelial cells were GFP positive (Fig. 4e). 7 days after wounding no GFP-positive fibroblasts were present in the wound bed (Fig. 4e; Fig. E10c-d) and at day 17 GFP-positive fibroblasts were exclusively detected immediately underneath the reformed epidermis (Fig. 4f; Fig. E10d).

We conclude that the first wave of dermal regeneration depends on cells of the reticular dermis and hypodermis, which are not capable of inducing hair follicles (Fig. 2i-k) and which elaborate the collagenous ECM characteristic of fibrosis⁶. The upper dermal lineage is not repopulated until re-epithelialisation and contributes exclusively to the papillary dermis. This explains both the rapid reconstitution of the skin adipocyte layer after wounding¹⁹ and the absence of hair follicles in newly closed wounds²⁰.

Sustained activation of the canonical Wnt pathway in adult epidermis induces growth of existing hair follicles (anagen), formation of new hair follicles^{21,22}, fibroblast proliferation and dermal ECM remodelling⁸. To examine the impact on the different dermal lineages we used K14 Δ N β -cateninER transgenic mice. One application of Tamoxifen induces anagen, while repeated applications stimulate ectopic hair follicle formation²¹. Epidermal β -catenin activation led to expansion of the upper and lower dermal compartments, the effects being more pronounced in mice that received multiple applications of Tamoxifen (Fig. 4h-k; Fig. E10e-g). The relative locations of the different dermal cells were unchanged (Fig. E9o-p). Expansion of the upper dermal lineage was evident in K14 Δ N β -cateninER x Blimp1Cre/CAGCATeGFP mice (Fig. 4g, h). Since epidermal Wnt signalling promotes hair follicle growth, the expansion of the lower dermis could explain why the skin adipocyte layer increases in thickness during anagen²².

To test whether epidermal β -catenin activation prior to wounding would promote hair follicle formation, K14 Δ N β -cateninER/Blimp1Cre/CAGCATeGFP mice were given repeated applications of Tamoxifen and subsequently wounded (Fig. 4l). This led to increased numbers of Itga8+ and Lrig1+ fibroblasts in the wound bed (Fig. 4m; Fig. E10h), an increased number of cells marked by Blimp1Cre (Fig. 4n) and a pronounced stimulation of hair follicle formation (Fig. 4o-q). We conclude that dermal remodelling in response to epidermal β -catenin activation leads to expansion of the upper and lower dermis, the increase in the upper papillary dermis being permissive for new hair follicle formation. It will be interesting to identify the downstream signalling pathways involved, one candidate being Hedgehog²¹. Wnt signalling regulates cells of the immune system²³ and a role for infiltrating $\gamma\delta$ T cells in promoting hair follicle formation has recently been described²⁴. The Wnt effector transcription factors Lef1 and Tcf3 were differentially expressed by upper and lower dermal fibroblasts (Fig. E5d-e), raising the intriguing possibility that different fibroblast lineages differ in their Wnt responsiveness and interactions with inflammatory cells²⁴.

In conclusion, the lineage hierarchies we have described reveal the cellular origins of the heterogeneous architecture of the dermis and provide a mechanistic basis for understanding the changes that take place during repair of adult skin wounds and in response to epidermal Wnt activation. We now have the opportunity to uncover events that result in dermal lineage specification, and discover how the different lineages contribute to the changes that occur during aging²⁵ and tumour formation¹.

Methods

Transgenic mice

Mice were maintained on a C57/Blk6 and CBA F1 background. PDGFRaCreER²⁸ or Dlk1CreERt (ICS) mice were bred with CAGCATeGFP²⁹ or ROSA26tdTomato (Jax Labs - 007905). PDGFRaeH2BeGFP mice³⁰ were obtained from Jackson Laboratories. Blimp1GFP¹⁴ and Blimp1Cre (Jax Labs - 008827)¹³ mice have been described previously. K14 Δ N β -cateninER mice have previously been described. Tamoxifen (Sigma Aldrich) was injected intraperitoneally into adult mice. 2mg of Tamoxifen in 100ul of acetone was administered topically to the back skin of pups. Bone marrow reconstitution experiments

and wounding (8 mm diameter full thickness wounds) were performed as described previously²⁶. All experiments were performed according to the guidelines of the UK Government Animals (Scientific Procedures) Act 1986 and underwent ethical review by Cambridge University and King's College London. Experiments were performed on female mice; however, the markers evaluated showed the same distribution in males. All experiments were performed on 3 or more female mice.

Flow cytometry

P2 disaggregated dermal preparations were prepared as previously described¹¹ and labelled with the antibodies listed below.

RT-PCR

This was performed as previously described²⁷. Analysis was performed by the delta-Ct method. Primer probe sets were purchased from Applied Biosystems and used according to manufacturer's recommendations: Ly6a/Sca1 - Mm00726565_s1; Dlk1/Pref1 - Mm00438422_m1; CD26/DPP4 - Mm00494538_m1; pparg -Mm01184322_m1; Zfp423 - Mm00473699_m1; Acta2 - Mm01546133_m1 Axin 2 - Mm01266783_m1; Dkk1 - Mm00438422_m1; Lef1 - MM01310389_m1; Tcf3 - Mm01188714_m1; Tcf712 - Mm00501505_m1; Wnt5a - Mm00437347_m1; Blimp1 - Mm01187285_m1.

Chamber grafting assay

This procedure was performed as previously described⁹. 8×10^6 wild type adult dorsal epidermal cells were combined with 5×10^6 wild type P2 dermal cells and 10^5 flow sorted PDGFRaH2BeGFP P2 dermal cells.

Histology and microscopy

5 μ m frozen sections and horizontal whole mounts were stained with the antibodies listed. The tissue array (Fig. 1c) was constructed from digitally excised images of areas of upper and lower dermis (Fig. 1b). All microscopy was performed on a Leica SP5 or Nikon A1 confocal microscope and images were analyzed in Image J and Adobe Photoshop CS6.

Horizontal whole mounts were prepared as previously described¹¹. Skin was collected and fixed in 4% PFA for 15-30 minutes then embedded in cryomolds. Sections were cut on a cryostat at a thickness of between 50-150 μ m. Instead of attaching sections with OCT onto slides, forceps were used to place sections into 1xPBS at room temperature. The 1xPBS dissolved away the OCT and tissue was then ready for staining in 300-500 μ l of PB buffer (1xPBS containing 0.5% skim milk, 0.25% Cold Water Fish Skin Gelatin, 0.5% Triton X100) in Eppendorf tubes. Sections could be stored for 3-6 months in 1xPBS at 4°C. Staining is subsequently performed by incubation with primary antibody overnight at 4°C on a rocker. Secondary antibodies were incubated for at least 2 hours at room temperature after 1 wash in 1xPBS for 1 hour. The tissue was then mounted on coverslips with a small volume of 100% glycerol and analysed by confocal microscopy.

Antibodies

The following antibodies were used: Itga8 (R&D Systems AF4076), Dlk1 (R&D Systems AF1144), CD26 (R&D Systems AF954), Sca1 (R&D Systems AF1226), PDGFRa (R&D Systems AF1062), Fabp4 (R&D Systems AF1443), AdipoQ (R&D Systems AF1119), Ephb3 (R&D Systems AF432), Lrig1 (R&D Systems AF3688), Podoplanin (R&D Systems AF3244), Transglutaminase2 (R&D Systems AF4376), Blimp1 (eBioscience 14-5963), CD26 (eBioscience 45-0261), Sca1 (eBioscience 56-5981-82), PDGFRa (eBioscience 14-140182), eCadherin (eBioscience 17-1449), CD34 (eBioscience 17-0349-42), CD44

(eBioscience 130441), CD45 (eBioscience 12-0451), CD31 (eBioscience 25-0311-82), GFP (Invitrogen A11122), LipidtoX (Rockland H34476), tdTomato (MBL 600-401-379), Dlk1 (Millipore D187-5), ColIV (Cell Signaling AB8201), Lef1 (Cell Signaling 2330S), Vimentin (Cell Signaling 5741S). The alpha-smooth muscle actin antibody was a gift from Frank Nestle, King's College London.

Clonal growth of fibroblast subpopulations in hydrogels

Flow sorted PDGFR α populations were seeded into Extracel hydrogels (Glycosan Biosystems, Salt Lake City, UT), which contain cross-linked gelatin and hyaluronic acid¹⁴, in individual wells of 24 well plates at a density of 5×10^4 cells per well. Cells were grown in Adipogenic Medium (R&D Systems) or standard Growth Medium (DMEM supplemented with 10% bovine serum) for 1 week. Cultures were fixed with 4% PFA, washed in PBS and stained with LipidtoX (Invitrogen 1:500) and DAPI. Spheres were scored positive for adipogenesis if they contained at least one lipid positive cell.

Graphing and Statistical Analysis

All graphs were generated using Excel, GraphPad Prism 6 and Adobe Illustrator CS4 software. Data are means \pm standard error of the mean (SEM). A One way ANOVA parametric test was performed for experiments with $P < 0.05$ considered significant.

Sample size for animal experiments was determined on the basis of pilot experiments. In the case of the skin reconstitution assays, animals were excluded from analysis only if grafts were unsuccessful (i.e. chamber falling out 1-2 days after grafting).

Supplementary Material

Refer to Web version on PubMed Central for supplementary material.

Acknowledgments

This work was funded by the Wellcome Trust (FMW, ACFS), the Medical Research Council (FMW, ACFS) and the European Union FP7 programme: TUMIC (FMW), HEALING (FMW) and EpigeneSys (ACFS). BML is the recipient of a FEBS long-term fellowship. KK is the recipient of a MRC PhD Studentship. The authors acknowledge financial support from the Department of Health via the National Institute for Health Research (NIHR) comprehensive Biomedical Research Centre award to Guy's & St Thomas' NHS Foundation Trust in partnership with King's College London and King's College Hospital NHS Foundation Trust. Input from Maria Mastrogiannaki, Andreas Reimer and Britta Trappmann is gratefully acknowledged. The authors also thank John Connelly and George Theodoridis for providing tissue and the KCL Hodgkins BSU staff, in particular Joan Castle, Claire Pearce and Dionne Cooper, for technical support.

References

1. Kalluri R, Zeisberg M. Fibroblasts in cancer. *Nat. Rev. Cancer.* 2006; 6:392–401. [PubMed: 16572188]
2. Gurtner GC, Werner S, Barrandon Y, Longaker MT. Wound repair and regeneration. *Nature.* 2008; 453:314–321. [PubMed: 18480812]
3. Martin P. Wound healing--aiming for perfect skin regeneration. *Science.* 1997; 276:75–81. [PubMed: 9082989]
4. Shah M, Foreman DM, Ferguson MW. Neutralising antibody to TGF-beta 1,2 reduces cutaneous scarring in adult rodents. *J. Cell Sci.* 1994; 107:1137–1157. [PubMed: 7929624]
5. Van Exan RJ, Hardy MH. The differentiation of the dermis in the laboratory mouse. *Am. J. Anat.* 1984; 169:149–164. [PubMed: 6711458]

6. Dulauroy S, Di Carlo SE, Langa F, Eberl G, Peduto L. Lineage tracing and genetic ablation of ADAM12(+) perivascular cells identify a major source of profibrotic cells during acute tissue injury. *Nat. Med.* 2012; 18:1262–1270. [PubMed: 22842476]
7. Janson DG, Saintigny G, van Adrichem A, Mahe C, El Ghalbzouri A. Different gene expression patterns in human papillary and reticular fibroblasts. *J. Invest. Dermatol.* 2012; 132:2565–2572. [PubMed: 22696053]
8. Collins CA, Kretzschmar K, Watt FM. Reprogramming adult dermis to a neonatal state through epidermal activation of beta-catenin. *Development.* 2011; 138:5189–5199. [PubMed: 22031549]
9. Jensen KB, Driskell RR, Watt FM. Assaying proliferation and differentiation capacity of stem cells using disaggregated adult mouse epidermis. *Nature Protocols.* 2010; 5:898–911.
10. Festa E, et al. Adipocyte lineage cells contribute to the skin stem cell niche to drive hair cycling. *Cell.* 2011; 146:761–771. [PubMed: 21884937]
11. Driskell RR, et al. Clonal growth of dermal papilla cells in hydrogels reveals intrinsic differences between Sox2-positive and -negative cells in vitro and in vivo. *J. Invest. Dermatol.* 2012; 132:1084–1093. [PubMed: 22189784]
12. Lesko MH, Driskell RR, Kretzschmar K, Goldie SJ, Watt FM. Sox2 modulates the function of two distinct cell lineages in mouse skin. *Dev. Biol.* 2013; 382:15–26. [PubMed: 23948231]
13. Robertson EJ, et al. Blimp1 regulates development of the posterior forelimb, caudal pharyngeal arches, heart and sensory vibrissae in mice. *Development.* 2007; 134:4335–4345. [PubMed: 18039967]
14. Horsley V, et al. Blimp1 defines a progenitor population that governs cellular input to the sebaceous gland. *Cell.* 2006; 126:597–609. [PubMed: 16901790]
15. Magnusdottir E, et al. Epidermal terminal differentiation depends on B lymphocyte-induced maturation protein-1. *Proc. Natl Acad Sci USA.* 2007; 104:14988–14993. [PubMed: 17846422]
16. Gomez C, Chua W, Miremadi A, Quist S, Headon DJ, Watt FM. The interfollicular epidermis of adult mouse tail comprises two distinct cell lineages that are differentially regulated by Wnt, Edaradd, and Lrig1. *Stem Cell Reports.* 2013; 1:19–27. [PubMed: 24052938]
17. Page ME, Lombard P, Ng F, Gottgens B, Jensen KB. The epidermis comprises autonomous compartments maintained by distinct stem cell populations. *Cell Stem Cell.* 2013 doi:10.1016/j.stem.2013.07.010.
18. Egawa G, Osawa M, Uemura A, Miyachi Y, Nishikawa S. Transient expression of ephrin b2 in perinatal skin is required for maintenance of keratinocyte homeostasis. *J. Invest. Dermatol.* 2009; 129:2386–2395. [PubMed: 19571816]
19. Schmidt BA, Horsley V. Intradermal adipocytes mediate fibroblast recruitment during skin wound healing. *Development.* 2013; 140:1517–1527. [PubMed: 23482487]
20. Ito M, et al. Wnt-dependent de novo hair follicle regeneration in adult mouse skin after wounding. *Nature.* 2007; 447:316–320. [PubMed: 17507982]
21. Silva-Vargas V, et al. Beta-catenin and Hedgehog signal strength can specify number and location of hair follicles in adult epidermis without recruitment of bulge stem cells. *Dev. Cell.* 2005; 9:121–131. [PubMed: 15992546]
22. Plikus MV, et al. Cyclic dermal BMP signalling regulates stem cell activation during hair regeneration. *Nature.* 2008; 451:340–344. [PubMed: 18202659]
23. Staal FJ, Luis TC, Tiemessen MM. WNT signalling in the immune system: WNT is spreading its wings. *Nat. Rev. Immunol.* 2008; 8:581–593. [PubMed: 18617885]
24. Gay D, et al. Fgf9 from dermal gammadelta T cells induces hair follicle neogenesis after wounding. *Nature Med.* 2013; 19:916–923. [PubMed: 23727932]
25. Giangreco A, Qin M, Pintar JE, Watt FM. Epidermal stem cells are retained in vivo throughout skin aging. *Aging Cell.* 2008; 7:250–259. [PubMed: 18221414]
26. Arwert EN, et al. Tumor formation initiated by nondividing epidermal cells via an inflammatory infiltrate. *Proc. Natl Acad. Sci. USA.* 2010; 107:19903–19908. [PubMed: 21041641]
27. Driskell RR, Giangreco A, Jensen KB, Mulder KW, Watt FM. Sox2-positive dermal papilla cells specify hair follicle type in mammalian epidermis. *Development.* 2009; 136:2815–2823. [PubMed: 19605494]

28. Rivers LE, et al. PDGFRA/NG2 glia generate myelinating oligodendrocytes and piriform projection neurons in adult mice. *Nature Neurosci.* 2008; 11:1392–1401. [PubMed: 18849983]
29. Kawamoto S, et al. A novel reporter mouse strain that expresses enhanced green fluorescent protein upon Cre-mediated recombination. *FEBS Letts.* 2000; 470:263–268. [PubMed: 10745079]
30. Hamilton TG, Klinghoffer RA, Corrin PD, Soriano P. Evolutionary divergence of platelet-derived growth factor alpha receptor signaling mechanisms. *Mol. Cell Biol.* 2003; 23:4013–4025. [PubMed: 12748302]

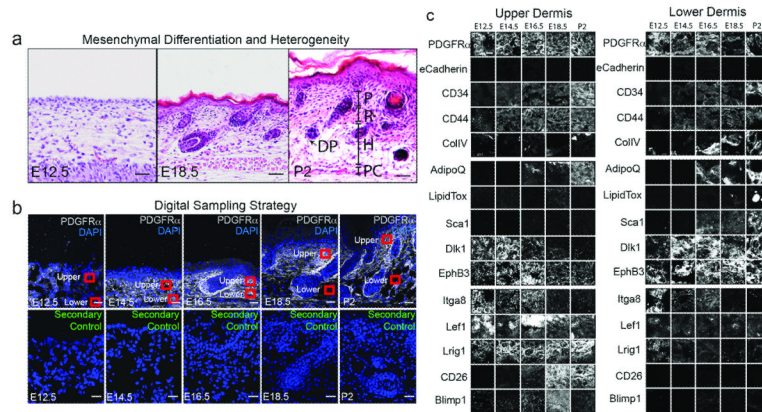


Figure 1. Morphological and molecular markers of embryonic and postnatal fibroblasts (a-c) Sections of mouse back skin. **(a)** H&E staining. P: papillary dermis; R: reticular dermis; H: hypodermis; P: panniculus carnosus; DP: dermal papilla. **(b)** 10 μ m sections immunostained with PDGFR α antibodies and secondary antibody control with DAPI nuclear counterstain. Red squares show areas digitally sampled for the tissue screen. **(c)** Tissue screen of upper and lower dermis. 3 biological replicates for each stain were performed. Images are representative samples of sections shown Fig. E1, E2. Scale bars: 50 μ m.

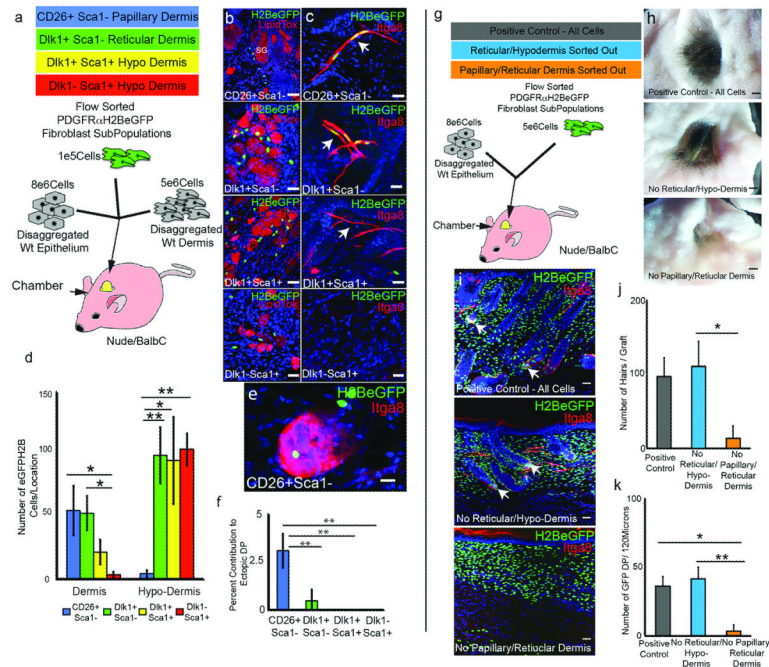


Figure 2. Skin reconstitution assays

(a) Experimental set up for (b-f). (b-c) Grafts immunostained with DAPI counterstain (blue). SG: sebaceous gland. Arrows: APM. (d-f) Contribution of PDGFR α H2BeGFP cells to dermal compartments. (g) Experimental set up for (h-k). (h) Macroscopic views of grafts. (i) Contribution of GFP⁺ cells to grafts. Arrows: GFP⁺ DP. (j) Hair follicles per graft. (k) GFP⁺ DP per 120 microns graft. N=3 biological replicates per experiment. *P < 0.05; **P < 0.005. Horizontal whole mounts shown. Scale bars: (b-c) 40 μ m (e) 30 μ m (h) 2.5mm (i) 50 μ m.

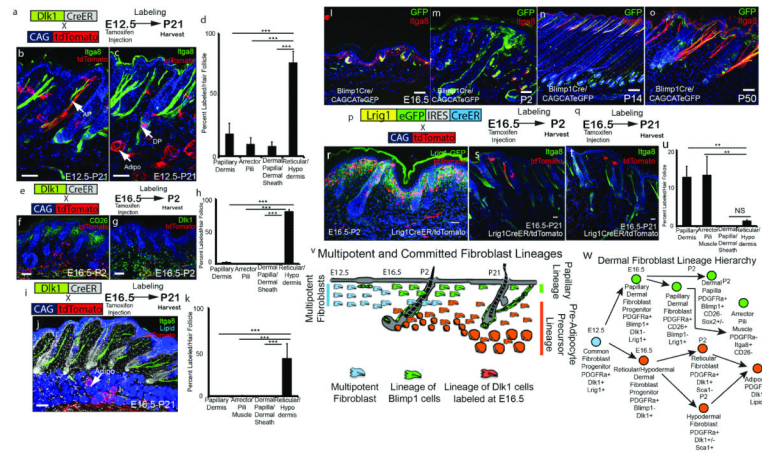


Figure 3. Fibroblast lineage commitment during skin development

(a, e, i, p, q) Labelling strategies. (b, c, f, g, j, l-o, r-t) Contribution of labelled cells to different dermal compartments. AP: arrector pili muscle; DP: dermal papilla; Adipo: adipocyte. (d, h, k, u) Average number labeled cells per unit area of dermis (defined by hair follicle spacing). (v, w) Schematic summary of lineage restriction. 3 biological replicates analyzed per experiment. Sections counterstained with DAPI. NS – Not statistically significant different; *P < 0.005, ***P < 0.0005. Scale bars: 50 μm.

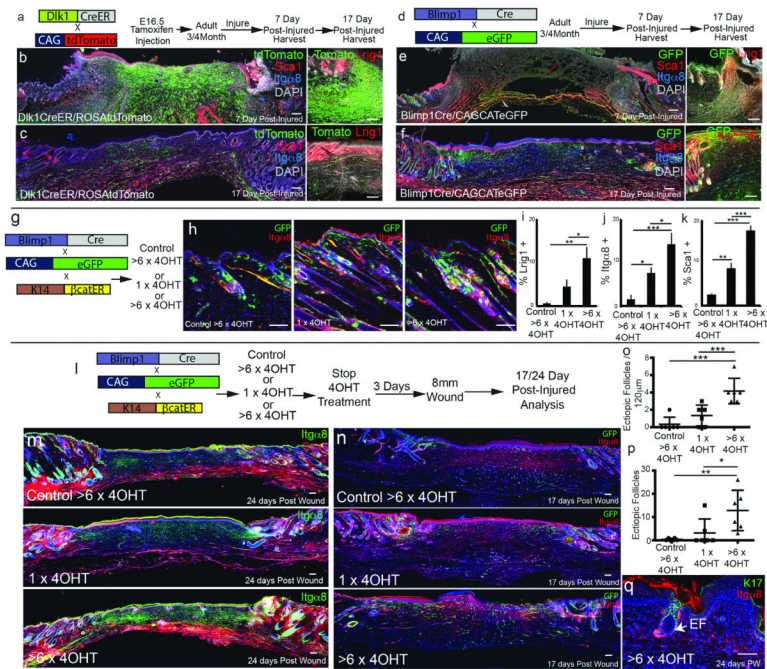


Figure 4. Contribution of fibroblast lineages in adult skin
(a, d, g, l) Labelling strategies. **(b, c, e, f, h, m, n, q)** Histological analysis of horizontal whole mounts. **(i-k)** Flow cytometric quantification of fibroblast markers. **(o, p)** Quantitation of ectopic hair follicles in **(o)** 17 day wound bed whole mount sections and **(p)** entire 24 day wound bed. (i-k) $n = 3$, (o, p) $n = 6$ biological replicates. * $P < 0.05$, ** $P < 0.005$, *** $P < 0.0005$. Scale bars: $200\mu\text{m}$ (b, c, e, f), $100\mu\text{m}$ (m, n, q) or $50\mu\text{m}$ (higher magnification views).